JOURNAL OF PHYSICAL ORGANIC CHEMISTRY
J. Phys. Org. Chem. 2006; **19:** 518–530
Published online 6 November 2006 in Wiley InterScience (www.interscience.wiley.com). DOI: 10.1002/poc.1051

Theoretical modeling of chemical reactions in complex environments: The intramolecular proton transfer in aqueous malonaldehyde†

Massimiliano Aschi,[1]* Marco D'Abramo,[2] Fabio Ramondo,[1] Isabella Daidone,[2] Maira D'Alessandro,[2] Alfredo Di Nola[2] and Andrea Amadei[3]**

[1]Dipartimento di Chimica, Ingegneria Chimica e Materiali, Università di L'Aquila, via Vetoio (Coppito 2), 67010 L'Aquila, Italia
[2]Dipartimento di Chimica, Universita' di Roma ''La Sapienza'', P.le Aldo Moro 5, 00185 Roma, Italia
[3]Dipartimento di Scienze e Tecnologie Chimiche Università di Roma ''Tor Vergata'', via della Ricerca Scientifica 00133 Roma, Italia

Received 18 October 2005; revised 3 February 2006; accepted 6 February 2006

ABSTRACT: The free energy profile and the (classical) kinetics of chemical reactions in (soft) condensed phase are modeled theoretically by means of molecular dynamics simulations, the Perturbed Matrix Method (PMM) and the quasi Gaussian entropy (QGE) theory. In this paper we describe the theoretical framework and apply the model to the intramolecular proton transfer reaction of aqueous malonaldehyde. Although in the present application we disregard the quantum effects for the proton dynamics along the reaction coordinate (i.e., tunneling), the classical-like view of the proton transition over the reaction free energy surface seems to properly describe the kinetic process and shows that water acts lowering the reaction free energy barrier. Moreover, a weak temperature dependence of the free energy surface is obtained, implying small entropy variations in the transition. Interestingly the activation entropy, as provided by the QGE model, is negative in the whole temperature range considered, thus indicating an entropy reduction at the transition structure. Finally, by comparing our results with theoretical and experimental literature data, we critically address the actual role of tunneling in this reaction and discuss the emerging kinetic scheme. Copyright © 2006 John Wiley & Sons, Ltd.

KEYWORDS: molecular dynamics; quantum mechanics; chemical kinetics; statistical mechanics

INTRODUCTION

Cis malonaldehyde (1) is the simplest beta-dicarbonyl compound which presents

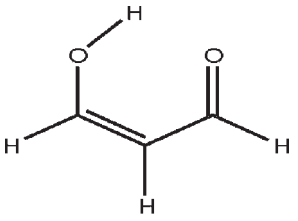

(1)

the essential features to study the intramolecular hydrogen bond and proton transfer kinetics and dynamics according to the reaction 1 reported in the following scheme.

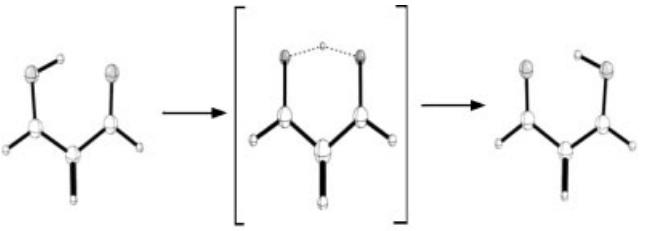

In the above reaction the Cs structures **1a** and **1b** unimolecularly transform into each other through the transition structure **1c** (C2v symmetry), as obtained by the vacuum minimum energy path defining the intrinsic reaction coordinate (IRC).[1]

In the gas phase, reaction I has been extensively studied and basically all the energetic[2–5] and dynamical[6–9] aspects have been clarified. The typical double well potential profile of this reaction has been ascertained from X-ray photoelectron[10,11] infrared[12–14] and microwave[15] spectroscopy. Moreover, the kinetics of this reaction has been also experimentally addressed in gas phase by studying the splitting of vibrational levels[16] and

**Correspondence to:* M. Aschi, Dipartimento di Chimica, Ingegneria Chimica e Materiali, University di l'Aquila, via Vetoio (Coppito 2), 67010 L'Aquila, Italia.
E-mail: aschi@caspur.it
***Correspondence to:* A. Amadei, Dipartimento di Scienze e Tecnologie Chimiche University di Roma ''Tor Vergata'', via della Ricerca Scientifica 00133 Roma, Italia.
E-mail: andrea.amadei@uniroma2.it
†Selected paper presented at the 10th European Symposium on Organic Reactivity, 25–30 July 2005, Rome, Italy.

estimating the energy barrier.[17] Differently from the gas phase, the knowledge on this reaction in solution is much more limited. First of all, despite of the large number of NMR experiments[18–20] and quantum-chemical calculations[5] with the Polarizable Continuum Model (PCM),[21] the actual stability of *cis* malonaldehyde is not well clarified, although the *trans* isomer should be the predominant form in water.

Second, the involvement of the light proton in the reaction may in principle provide relevant quantum effects even in condensed phase.

All these complications did not prevent this reaction to be used as a prototypical system for theoretical studies of intramolecular proton transfer in condensed phase.[22–26]

Finally, and most importantly, the modeling of chemical reactions in complex environment (solution) still represents a challenge for theoretical-computational chemistry.[27–30]

In this respect the main aim of this work is to introduce (and evaluate the reliability of) an alternative theoretical approach providing a tool, complementary to existing computational schemes, for addressing chemical reactions in solution. As a matter of fact in this paper we evaluate the reaction free energy surface of the reaction I in water, by means of a theoretical model based on statistical mechanics and the perturbed matrix method (PMM),[31–37] as introduced[38] and applied[39] in very recent papers. Moreover, using the quasi Gaussian entropy (QGE) theory[40] to model the reaction free energy in temperature, we are able to construct a complete theoretical description of the reaction thermodynamics. Finally, evaluating the diffusion coefficient along the reaction coordinate we also obtain the (classical) kinetics of the chemical process in solution and hence, comparing our results with the available experimental and theoretical literature data, we address the problem of the role of tunneling in this reaction.

THEORY

In condensed phase multiple minimum energy reaction paths are present and hence the definition of the reaction coordinate is not as simple as in gas phase, where for rigid or semi-rigid molecules a unique IRC can be usually defined.[41–44]

In principle one might search for the minimum free energy path in configurational space, that is, the unidimensional curve such that at each position the free energy obtained within the plane orthogonal to the curve is the minimum possible. However such an evaluation, even for a simple molecule like malonaldehyde, is virtually impossible. Moreover, it must be noted that several reaction coordinates are in principle possible to be used to correctly describe the reaction kinetics, in particular for a condensed phase system, which involves a huge number of degrees of freedom. In fact, in order to define a proper (single) reaction coordinate for describing the kinetics of the chemical process and not only its thermodynamics, we need to use a classical degree of freedom such that all its orthogonal coordinates are well equilibrated during its relaxation.[45] Hence, it is possible that according to the initial conditions of the kinetic relaxation (i.e., the coordinates/observables equilibrated at the beginning of the process) and the exact definition of the reactant and product states, different reaction coordinates should be used. This clearly implies that a certain variation of the reaction free energy profile is possible, as a consequence of the different choice of the reaction coordinate and hence of the orthogonal planes used to obtain the corresponding free energy. In principle, each of these reaction coordinates, if properly defined, should provide the correct (classical) kinetic relaxation for the corresponding process. In the present study we consider the IRC, evaluated in vacuum and resulted as a linear generalized degree of freedom (i.e., it is defined by a single unit vector in configurational space), as the proper reaction coordinate also in condensed phase. The use of IRC for describing the proton transfer kinetics, can be motivated by the rather high frequencies found for the orthogonal internal motions *in vacuo*. This means that also in condensed phase, where the perturbation effect on high frequency vibrations is expected to be weak,[46] we may assume that the kinetic (classical) relaxation along IRC occurs with all the other degrees of freedom equilibrated, that is, the kinetics along IRC may be modeled as a diffusion along the free energy surface. Note that, for a highly diluted solute, the reaction free energy is independent of the solute roto-translational coordinates[38] and the solvent, provided an initial equilibrium condition, is expected to relax instantaneously in the ensemble of reactive trajectories at each reaction coordinate position (see the Results and Discussion section). However, it must be remarked that for a light particle like a proton, a purely classical diffusion onto the reaction free energy surface could be not sufficient to describe the complete kinetics of the process, where tunneling effects might be present. In this paper we disregard such quantum effects and hence the model used provides the reaction free energy surface and the corresponding diffusion process, as obtained by PMM and (classical) molecular dynamics (MD) simulations.

Defining with $\boldsymbol{r}_n$ the nuclear coordinates of the quantum center (QC) (i.e., the system treated quantum mechanically) and $\boldsymbol{r}$ the coordinates of the atoms providing the (classical) perturbing field we can write, within certain approximations,[32,34] the QC electronic (perturbed) Hamiltonian matrix as

$$\tilde{H}(\boldsymbol{r}_n,\boldsymbol{x}) \cong \tilde{H}^0(\boldsymbol{r}_n) + q_T V(\boldsymbol{r}_0,\boldsymbol{x})\tilde{I} + \tilde{Z}_1(\boldsymbol{E}(\boldsymbol{r}_0,\boldsymbol{x}),\boldsymbol{r}_n) + \Delta V(\boldsymbol{r}_n,\boldsymbol{x})\tilde{I} \quad (1)$$

where $\tilde{H}^0(\boldsymbol{r}_n)$ is the unperturbed Hamiltonian matrix which can be constructed carrying out standard electronic structure calculations on the isolated QC, $V(\boldsymbol{r}_0,\boldsymbol{x})$ and $\boldsymbol{E}(\boldsymbol{r}_0,\boldsymbol{x})$ are the (perturbing) electric potential and electric

field at a given QC $\boldsymbol{r}_0$ position (typically the geometrical center), $\tilde{Z}_1(\boldsymbol{E}, \boldsymbol{r}_n)$ is a perturbation matrix explicitly given by $[\tilde{Z}_1]_{l,l'} = -\boldsymbol{E} \cdot \langle \Phi_l^0 | \hat{\boldsymbol{\mu}} | \Phi_{l'}^0 \rangle$, where $\hat{\boldsymbol{\mu}}$ is the electric dipole operator. In the above equation $\Delta V(\boldsymbol{r}_n, \boldsymbol{x})$ approximates the perturbation due to all the higher order terms as a simple short range potential and q_T is the QC total charge. Moreover, Φ_l^0 are the unperturbed (electronic) Hamiltonian eigenfunctions and all the matrices used are expressed in this unperturbed basis set. At each MD frame, the electric potential and field exerted by the environment can be simply evaluated (typically using the environment atomic charge distribution) and the perturbed Hamiltonian matrix constructed and diagonalized. Hence, a trajectory of the QC perturbed eigenvalues and eigenvectors is obtained. Such calculations carried out along the reaction coordinate provide, within certain approximations and for a highly diluted QC,[38] the reaction free energy and whatever electronic property at a generic reaction coordinate position η. According to the theoretical model described in the previous paper,[38] the (Helmholtz) free energy change for the reaction coordinate transition $\eta_R \rightarrow \eta$ (providing the reaction standard chemical potential $\Delta\mu^{\ominus}$ as in our calculation the solute density is invariant along the transition) and the average value of an electronic property χ at the position η, are

$$\Delta A(\eta) = \Delta\mu^{\ominus}(\eta) \cong -kT \ln \left\langle \mathrm{e}^{-\beta\Delta(\varepsilon' + q_T V)} \right\rangle_{\eta_R}^{0} \tag{2}$$

$$\langle \chi(\eta) \rangle \cong \frac{\left\langle \mathrm{e}^{-\beta\Delta(\varepsilon' + q_T V)} \chi(\eta) \right\rangle_{\eta_R}^{0}}{\left\langle \mathrm{e}^{-\beta\Delta(\varepsilon' + q_T V)} \right\rangle_{\eta_R}^{0}} \tag{3}$$

In the previous equations ε' is the (ground state) eigenvalue of $\tilde{H}^0 + \tilde{Z}_1$ and $\Delta(\varepsilon' + q_T V)$ provides the energy change, for each MD frame, due to the transition along the reaction coordinate and obtained energy minimizing the QC internal quantum degrees of freedom. Moreover, the subscript η_R and the zero superscript mean that the averages are performed in the statistical ensemble with constrained reaction coordinate (at the reactant structure position η_R) and QC rototranslational motions, where the system (a single QC and the water molecules) is in its vibrational ground state. The previous expressions are correct within the approximation that a small reactant to product displacement along the reaction coordinate, does not affect the quantum vibrations and (classical) mass tensor determinant.[38] Moreover, as malonaldehyde is a rather rigid molecule we may consider that, for each solvent configuration, $\Delta(\varepsilon' + q_T V)$ is a function only of the reaction coordinate, that is, it is independent of the other QC internal coordinates, and hence only the structures along the minimum energy path (obtained *in vacuo*) are necessary to provide the unperturbed properties for PMM calculations along IRC.[38] In the special case we deal with an isolated QC the previous expression for the reaction free energy reduces to the unperturbed QC electronic ground state energy variation obtained by the unperturbed Hamiltonian matrix $\tilde{H}^0$ evaluated along the reaction coordinate.

In this paper, where we consider all the QC internal coordinates orthogonal to IRC as harmonic (quantum) degrees of freedom and the proton transfer is defined by a relatively large IRC transition, it may be worth to evaluate the correction term providing the free energy change at η, due to the possible variation of the vibrational energies and (classical) mass tensor determinant from the corresponding values at η_R. Assuming, as usual, the partition function as factorized into a semi-classical part and a quantum vibrational one (given by the product of the molecular vibrational partition functions) and considering rigid solvent molecules (water) with hence a coordinate independent classical mass tensor, we may express such a free energy term $\Delta A_I(\eta)$ as[38,40]

$$\Delta A_I(\eta) \cong - kT \ln \frac{Q_{v,\eta} \int \mathrm{e}^{-\beta\left[\Phi(\mathrm{x},\eta) + \Delta u_{v,0}(\mathrm{x},\eta)\right]} \left[\det \tilde{M}(\eta)\right]^{1/2} \mathrm{d}\boldsymbol{x}}{Q_{v,\eta_R} \int \mathrm{e}^{-\beta\left[\Phi(\mathrm{x},\eta) + \Delta u_{v,0}(\mathrm{x},\eta_R)\right]} \left[\det \tilde{M}(\eta_R)\right]^{1/2} \mathrm{d}\boldsymbol{x}} \tag{4}$$

where $Q_{v,\eta}$, Q_{v,η_R} are the QC molecular quantum vibrational partition functions including all the orthogonal internal degrees of freedom, obtained at η and η_R, respectively, and $\boldsymbol{x}$ are the solvent (classical) coordinates. Moreover, $\tilde{M}(\eta)$ and $\tilde{M}(\eta_R)$ are the mass tensors associated to all the QC classical coordinates (i.e., rototranslational and IRC coordinates) as obtained at η and η_R, Φ is the (classical) potential energy of the system (QC plus environment), and $\Delta u_{v,0}$ is the system vibrational ground state energy shift from a reference value,[38,40] due to the solvent interaction and typically negligible. In malonaldehyde all the internal coordinates orthogonal to IRC are characterized by rather high frequencies and hence are considered as quantum degrees of freedom, classically equivalent to constrained coordinates, described by the vibrational partition function. Therefore, in Eqn (4) no integration over QC classical coordinates is present. Note also that the use of the QC complete classical mass tensor determinant implies that, as required in Eqn (4), we deal with the unconstrained ensemble.[38] Using the approximation $\Delta u_{v,0}(\mathbf{x}, \eta) \cong \Delta u_{v,0}(\boldsymbol{x}, \eta_R)$ we then obtain, for the perturbed (solvated) or isolated QC,

$$\Delta A_I(\eta) \cong -kT \ln \frac{Q_{v,\eta}}{Q_{v,\eta_R}} - \frac{kT}{2} \ln \frac{\det \tilde{M}(\eta)}{\det \tilde{M}(\eta_R)} \tag{5}$$

providing

$$\Delta A(\eta) = \Delta\mu^{\ominus}(\eta) \cong -kT \ln \left\langle \mathrm{e}^{-\beta\Delta(\varepsilon' + q_T V)} \right\rangle_{\eta_R}^{0} - kT \ln \frac{Q_{v,\eta}}{Q_{v,\eta_R}} - \frac{kT}{2} \ln \frac{\det \tilde{M}(\eta)}{\det \tilde{M}(\eta_R)} \tag{6}$$

where the QC vibrational partition function along the reaction coordinate can be in general obtained via the corresponding *in vacuo* frequencies, that is, we consider

the unperturbed frequencies as the reference frequencies used in the definition of the vibrational partition function.[38,40] Note that within the approximations used to obtain ΔA_I, no corrections are needed for the χ average. We can obtain further useful relations expressing the reaction free energy via the excess (Helmholtz) free energy $A' = A - A_{\mathrm{ref}}$ (A_{ref} is the free energy of a proper reference condition[40] defined at the same temperature and density of the actual system but with $\Phi + \Delta u_{v,0} = 0$)

$$\Delta A(\eta) = A'(\eta) - A'(\eta_R) + A_{\mathrm{ref}}(\eta) - A_{\mathrm{ref}}(\eta_R) \tag{7}$$

$$A'(\eta) = kT \ln\left\langle e^{\beta u'(\boldsymbol{x},\eta)}\right\rangle - kT \ln \varepsilon_\eta \tag{8}$$

$$A'(\eta_R) = kT \ln\left\langle e^{\beta u'(\boldsymbol{x},\eta_R)}\right\rangle - kT \ln \varepsilon_{\eta_R} \tag{9}$$

$$A_{\mathrm{ref}}(\eta) - A_{\mathrm{ref}}(\eta_R) = -kT \ln\frac{Q_{v,\eta}}{Q_{v,\eta_R}} - \frac{kT}{2}\ln\frac{\det\tilde{M}(\eta)}{\det\tilde{M}(\eta_R)} \tag{10}$$

$$u'(\boldsymbol{x},\eta') = \Phi(\boldsymbol{x},\eta') + \Delta u_{v,0}(\boldsymbol{x},\eta') \tag{11}$$

where the averages are defined in the fixed η and η_R (unconstrained) vibrational ground state ensembles[40] and ε_η, ε_{η_R} are the corresponding confinement fractions as defined in the QGE theory. Using $\Delta A'(\eta) = A'(\eta) - A'(\eta_R)$, Eqns (6), (7), and (10) we then have

$$\Delta A'(\eta) = \Delta\mu'(\eta) \cong -kT \ln\left\langle e^{-\beta\Delta(\varepsilon' + q_T V)}\right\rangle_{\eta_R}^{0} \tag{12}$$

$$\Delta\mu'(\eta) = \mu'(\eta) - \mu'(\eta_R) \tag{13}$$

where the excess chemical potential μ' can be expressed by the QGE Gamma state model which proved to be very accurate for solute-solvent systems[40]

$$\mu' = u'_0 - T_0 c'_{V_0}\Lambda(T) - kT\ln\bar{\varepsilon} + p'v$$
$$\Lambda(T) = \frac{1}{\delta_0} + \frac{T}{T_0\delta_0^2}\ln\left[\frac{T(1-\delta_0)}{T(1-\delta_0) + T_0\delta_0}\right] \tag{14}$$

with u'_0, c'_{V_0} the solute partial molecular excess internal energy and heat capacity at the reference temperature T_0, δ_0 a temperature-independent intensive property that like the excess pressure p' *i*s defined only by the solvent, $k\ln\bar{\varepsilon}$ the solute partial molecular confinement entropy and v the solute partial molecular volume. For a chemical reaction like malonaldehyde proton transfer we may safely assume that both $k\ln\bar{\varepsilon}$ and v are independent of the IRC position and hence

$$\Delta\mu^{\ominus}(\eta) \cong \Delta u'_0(\eta) - T_0\Delta c'_{V_0}(\eta)\Lambda(T) - kT\ln\frac{Q_{v,\eta}}{Q_{v,\eta_R}} - \frac{kT}{2}\ln\frac{\det\tilde{M}(\eta)}{\det\tilde{M}(\eta_R)} \tag{15}$$

$$\Delta u'_0(\eta) = u'_0(\eta) - u'_0(\eta_R)$$
$$\Delta c'_{V_0}(\eta) = c'_{V_0}(\eta) - c'_{V_0}(\eta_R)$$

These last equations were used to obtain the complete reaction thermodynamics. Finally, using the reaction free energy profile and the diffusion coefficient D of the reaction coordinate (if available), it is possible to obtain the reaction (classical) kinetics by solving a diffusion equation[47] in the reaction coordinate space (see Appendix 2)

$$\left(\frac{\partial\rho}{\partial t}\right)_\eta = \frac{D}{kT}\left[\rho\left(\frac{\partial^2\Delta\mu^{\ominus}}{\partial\eta^2}\right)_t + \left(\frac{\partial\Delta\mu^{\ominus}}{\partial\eta}\right)_t\left(\frac{\partial\rho}{\partial\eta}\right)_t\right] + D\left(\frac{\partial^2\rho}{\partial\eta^2}\right)_t \tag{16}$$

where $\rho(t,\eta)$ is the probability density in η and we assumed $\partial D/\partial t, \partial D/\partial\eta \cong 0$.

QUANTUM CHEMICAL CALCULATIONS AND MOLECULAR DYNAMICS SIMULATIONS

All the quantum chemical calculations on the isolated malonaldehyde, that is our quantum center, were carried out by the Gaussian 98 package.[53] We have initially determined the essential features of the potential energy hypersurface characterizing the reaction I *in vacuo*, namely the potential energy minima (**1a**, **1b**) and the interconnecting first order saddle point (**1c**). In order to obtain the corresponding energies, we used Density Functional Theory (DFT) employing the Becke's three parameters[48] exchange and the Lee, Yang and Parr[49] correlation functionals (B3LYP) in conjunction with the 6-311 ++ G(p,d) atomic basis set.[50] The above calculations have been also repeated using the second order perturbation theory, that is, MP2 (full) level of theory, with the same atomic basis set. Coupled cluster theory including single, double and a perturbative estimate of triple excitations, that is, CCSD(T),[51] was finally applied to the B3LYP/6-311 ++ G(p,d) geometries to improve the quality of the energies of the minima and transition structures. These latter calculations are hereafter denoted as CCSD(T)/6-311 ++ G(p,d)//B3LYP/6-311 ++ G(p,d). The minimum energy path of reaction I was studied at the CCSD(T)/6-311 ++ G(p,d)//B3LYP/6-311 ++ G(p,d) level of theory by means of the Intrinsic Reaction Coordinate starting from the previously located transition structure **1c** and moving toward both minima **la** and **1b**. For each point along IRC we also evaluated the B3LYP/6-311 ++ G(p,d) mass-weighted Hessian matrix corresponding to the internal degrees of freedom orthogonal

to the reaction coordinates, that is, without including the reaction coordinate,[43] which provided the reference frequencies to be used in the vibrational partition function. In order to apply PMM at each structure of this path, the electronic ground and excited energies as well as the corresponding (transition) dipoles, were obtained at two levels of theory: Configuration Interaction with Single (electron) excitations (CIS) with 6-311 ++ G(p,d) atomic basis set, and Time Dependent Density Functional Theory (TD-DFT)[52] with B3LYP functional and the same atomic basis set. Both procedures provided virtually identical results and hence for PMM calculations presented here we utilized TD-DFT data. Note that in correspondence of each point of the IRC grid, that is, the QC structures along the reaction coordinate, ten states (i.e., the ground plus nine excited states) were optimized for the unperturbed QC, both at CIS and TD-DFT levels of theory. Such unperturbed Hamiltonian eigenstates defined the basis set used to construct the perturbed Hamiltonian matrix, Eqn (1), which was then diagonalized at each simulation frame, leading to the reaction free energy and related properties.

To evaluate the reaction free energy surface in solution MD simulations were performed over a wide temperature range (280–1200 K), constraining the reactant malonaldehyde (essentially the la structure) in the center of the simulation box, filled with 256 simple point charge (SPC)[54] water molecules, at the typical liquid density (55.32 mol/L). The parameters describing the reactant malonaldehyde force field were determined as follows: the charges were recalculated adopting several fitting procedures[55] and different levels of theory, namely DFT and MP2, to ascertain the stability of the results; for the other non-bonding and all the bonding interactions, inspired by previous articles on similar systems,[26] we used the parameters contained in the Gromos force field[59] designed for similar atoms. Note that within the force field used the overall energy minimum, if removing the interaction with the solvent, is defined by the **1a** structure (the minimum energy reactant geometry as obtained by the quantum chemical calculations in vacuum). Finally, malonaldehyde bond lengths were constrained by LINCS[60] and the rototranslational constraints[61] were used to keep the molecule rototranslationally fixed at the center of the simulation box. Such a constrained simulation procedure, providing the correct statistical mechanics and thermodynamics of a semi-rigid molecule[61] like malonaldehyde, is computationally convenient and allows a simple PMM application. Moreover, it is consistent with the physical model involved in Eqns (2) and (3): a rigid molecule with constrained rototranslational degrees of freedom. The choice of treating in the MD simulation the angular QC internal coordinates as stiff classical harmonic degrees of freedom instead of constrained ones, with hence the reaction coordinate also not exactly constrained at the reactant position, is motivated by the faster solvent relaxation occurring when the angular internal coordinates have some vibrational freedom. Such tiny angular and IRC fluctuations are negligible for the (equilibrium) statistical mechanical solvent behavior and hence the perturbing field distribution, as obtained by the MD simulation and used in PMM calculations, is virtually identical to the one obtained by a simulation with a fully constrained malonaldehyde. The temperature was kept constant using the isokinetic temperature coupling[62] to obtain results fully consistent with statistical mechanics.[61,63] For all the simulations the number of steps was 3 000 000 with three different time steps: 2 fs for simulations in the range 280–450 K, 1 fs in the range 450–800 K, and 0.5 fs in the range 800–1200 K. The long range electrostatics was calculated using the Particle Mesh Ewald (PME) method,[56] with 34 wave vectors in each dimension and a 4th order cubic interpolation. All the simulations were performed using the Gromacs package.[57–59]

To explicitly evaluate the (classical) kinetics of the proton transfer (provided by the diffusion along the reaction free energy surface), we first evaluated the diffusion coefficient associated to the IRC in the solvated reactant malonaldehyde. For this purpose we performed (by Gromacs) a 110 ps MD trajectory at constant energy (i.e., with no temperature coupling) of solvated reactant malonaldehyde, utilizing unconstrained bond lengths (with the corresponding Gromacs stretching parameters) and thus a reduced time step of 0.1 fs, starting from a MD frame of a similar simulation at 300 K (i.e., with the isokinetic temperature coupling), chosen so that its total energy was virtually identical to the value obtained by averaging over the 300 K simulation. For the rest, these simulations were performed identically to the previous ones. Note that in both simulations the first 10 ps were considered as equilibration and hence removed from the analysis. Finally, projecting a large number of the (constant energy) trajectory subparts starting close to the IRC free energy minimum (the reactant position η_R) onto the unit vector defining the reaction coordinate, we evaluated the diffusion coefficient of IRC via the corresponding computed mean square displacement in time. Note that for a fast velocity autocorrelation function relaxation, as in the present case where the diffusive regime is achieved within 1 fs, the use of a constant energy simulation to evaluate the diffusion coefficient is physically more consistent than using a constant temperature one. The obtained diffusion coefficient was then utilized to solve (numerically) the diffusion equation (note that we assume an IRC independent diffusion coefficient which then may be obtained considering only the reactant ensemble). The use of unconstrained internal coordinates, described in the last simulations by stiff classical harmonic vibrations around the la structure, is motivated by the need of evaluating the average dynamical behavior of the reaction coordinate via a purely classical model. For this purpose, to describe the possible dynamical coupling between internal coordinates,

we were forced to utilize classical vibrations with proper frequencies, that is, similar to the *ab initio* ones, and remove the constraints used for the statistical mechanical derivations where no dynamical information was required. Note that rototranslational motions can be considered as fully (dynamically) decoupled from IRC diffusion because of the extremely fast velocity autocorrelation function relaxation, and hence the use of the corresponding constraints in the simulation should have no effect on evaluating the diffusion coefficient.

RESULTS AND DISCUSSION

Malonaldehyde is a rather rigid molecule with a high energy dihedral barrier (about 65 kJ/mol or more in vacuum, at CCSD(T)).

To ascertain the reliability of choosing as QC the uncomplexed malonaldehyde, we systematically compared in vacuum the potential energy (i.e., the electronic ground state energy) profiles of reaction I considering some small but suitable la–water complexes (i.e., we tested possible reaction paths involving water proton exchange). In Table 1 we report the energy barrier heights for the proton transfer in such malonaldehyde–water complexes at different levels of theory. The reaction in vacuum, with no water molecules involved, presents a B3LYP barrier of 13.6 kJ/mol. At the CCSD(T)/6-311 ++ G(p,d)//B3LYP/6311 ++ G(p,d) level the value of the barrier is increased up to 18.1 kJ/mol in very good agreement with literature computational and experimental results.[2,17] Remarkably the B3LYP barriers obtained for all the complexes with water, result as invariably higher. Assuming a systematic underestimation of the B3LYP energy barriers with respect to the more computationally demanding CCSD(T)/6-311 ++ G(p,d), + G(p,d), such a result suggests that no water proton exchange is involved in malonaldehyde intramolecular proton transfer and, hence, that the uncomplexed malonaldehyde may provide a proper QC for PMM calculations. Interestingly, as mentioned in the previous sections, IRC is linear and hence defined by a single unit vector in configurational space. In Fig. 1 we show the atomic components of such unit vector, given by the square root of the sum of the corresponding x,y,z square components. Using the unit vector components and the atomic masses it is also possible to evaluate the mass associated to the reaction coordinate (i.e., the mass tensor diagonal element corresponding to IRC), which resulted of 3.1 a.u. The reaction free energy in solution along the IRC was obtained via PMM calculations based on the B3LYP procedure which in vacuum provided an underestimated energy barrier. Hence, assuming that at each η

Table 1. Proton transer barrier heights (kJ/mol) for malonaldehyde-$(H_2O)_n$, complexes ($n = 0$, 1, 2), in vacuum, calculated at the B3LYP/6-311 ++ G(d,p) (DFT), MP2/6311 ++ G(d,p) (MP2) and CCSD(T)/6-311 ++ G(d,p)//B3LYP/6-311 ++ G(d,p) (CC) levels of theory

Method	$n = 0$	$n = 1$	$n = 2$
DFT	13.4	22.5	75.1
MP2	13.6		
CC	18.1		

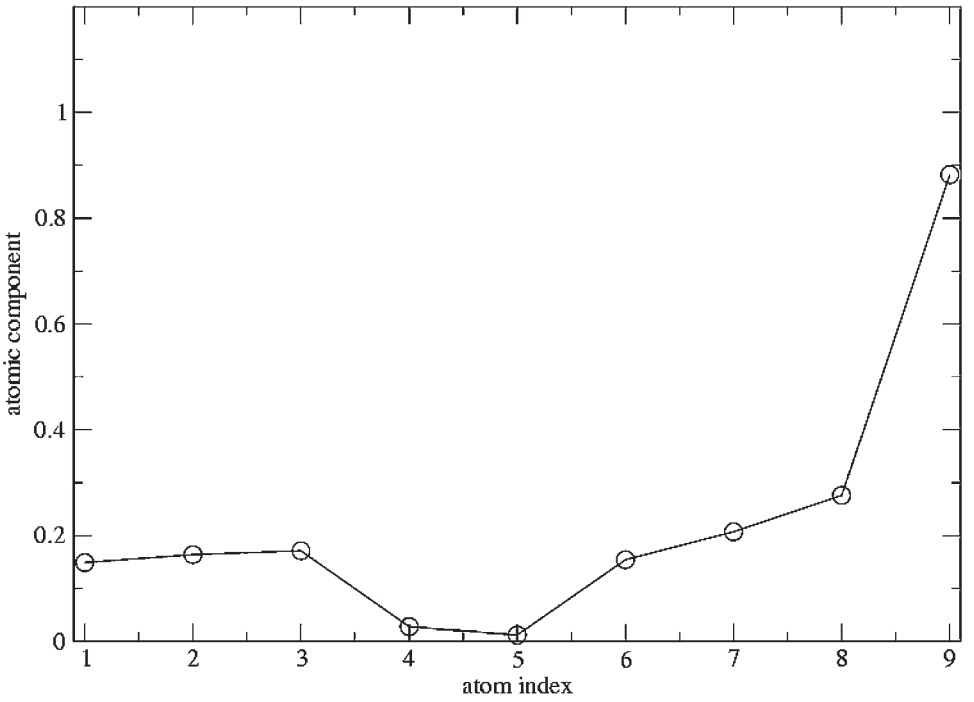

Figure 1. Atomic components (see text) of the unit vector defining the IRC

value the PMM/B3LYP reaction free energy subtracted of the corresponding (B3LYP) unperturbed contribution provides a more accurate evaluation, we obtained the (solution) reaction free energy surface adding such shifts to the CCSD(T) vacuum free energy surface. Note that the vibrational partition functions were obtained by the B3LYP vacuum frequencies and $\Delta A_I(\eta)$ resulted irrelevant in the whole IRC range considered. In Fig. 2 we report the perturbed free energy surface, as obtained by PMM and the MD simulation at 300 K, together with the CCSD(T) vacuum free energy profile and the 300 K reaction free energy as obtained by PCM using the same procedure and level of quantum chemical calculations (i.e., adding the PCM/B3LYP free energy shifts to the CCSD(T) curve). It is evident from PMM results that the solvent provides a free energy barrier (activation free energy) of about 2 kJ/mol lower than the vacuum one. Such a result, indicating a transition state (TS) solvation free energy larger than the reactant-product one, is expected from the (gas-phase) larger TS dipole moment. Note that this finding, valid for *cis* malonaldehyde proton transfer, does not necessarily apply to the overall proton transfer reaction, including the *cis–trans* equilibrium because of the relative thermodynamic instability of the *cis* isomer. PCM reaction free energy profile, although showing a similar shape to the PMM curve, presents a free energy barrier slightly higher than the vacuum one and predicts a local minimum in correspondence of the vacuum transition structure. Such an unphysical condition is probably due to the macroscopic dielectric polarization used in PCM to model solute-solvent interaction, which may be rather unrealistic as previously reported.[34,37] A further intriguing aspect, emerging by our model, is the fact that the free energy surface is only slightly affected when temperature is increased from 300 K to 1200 K, thus indicating a very limited entropic contribution to the reaction free energy. This is shown in Fig. 3 where we report the (PMM) activation free energy $\Delta\mu^{\ominus}(\eta_{TS})$ as a function of the temperature. In Fig. 3 we also show the curve obtained by using the QGE theory[40] to model PMM reaction free energy according to Eqn (15). The QGE model, accurately reproducing the PMM free energy barriers, provides also the corresponding activation entropy curve $\Delta s^{\ominus}(\eta_{TS})$, resulting in the whole temperature range between -1.3 and -0.2 J/(mol K) (see Fig. 3). Such small activation entropies indicate that no relevant solvent reorganization is present in the proton transfer, although the transition structure is always associated to a lower entropy. Interestingly, the free energy maximum position along the reaction coordinate is also virtually independent of the temperature, and hence it is always associated to the same molecular structure (data not shown).

To obtain the kinetics of the proton transfer reaction in aqueous malonaldehyde, within the classical view of the diffusion along the reaction free energy surface, we first evaluated the reaction coordinate diffusion coefficient, for a kinetic process occurring in water at 300 K (see previous section). In Fig. 4 we show the IRC mean square displacement (MSD) in time, as obtained by the constant

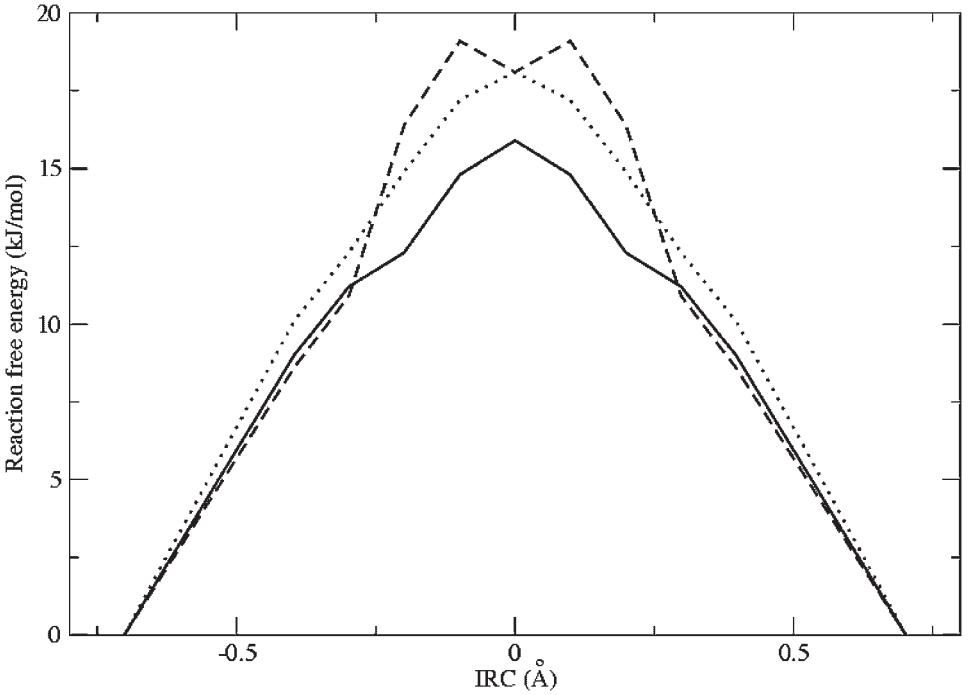

Figure 2. Reaction free energy surfaces as provided by PMM and the MD simulation at 300 K (solid line), CCSD(T) (vacuum) calculations (dotted line) and 300 K PCM calculations (dashed line)

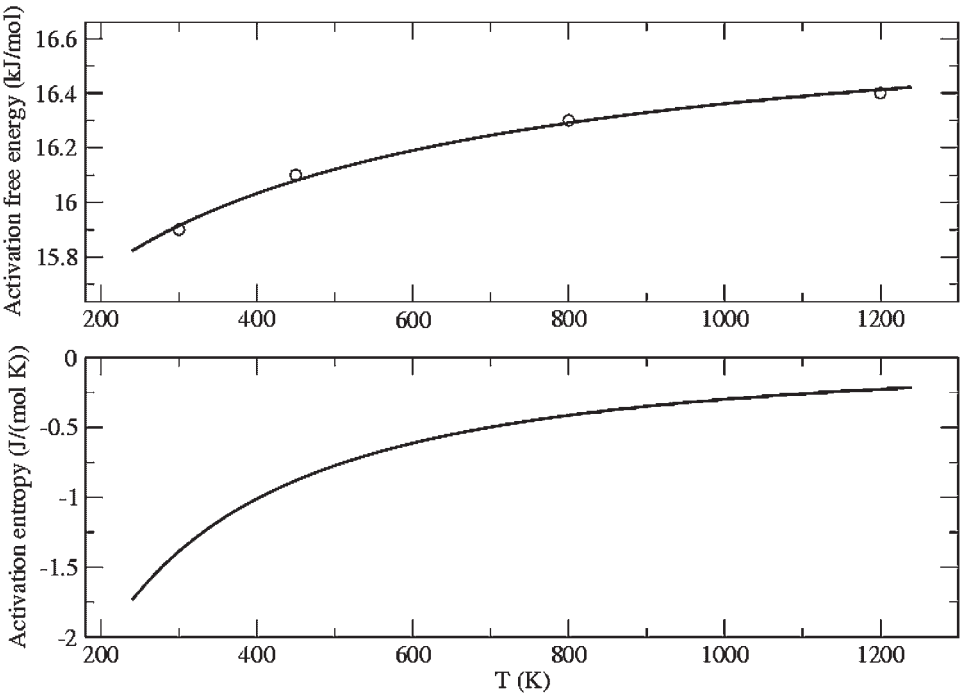

Figure 3. Activation free energy and entropy as provided by the QGE model (solid lines) and activation free energy obtained by PMM/MD results (circles) as a function of temperature

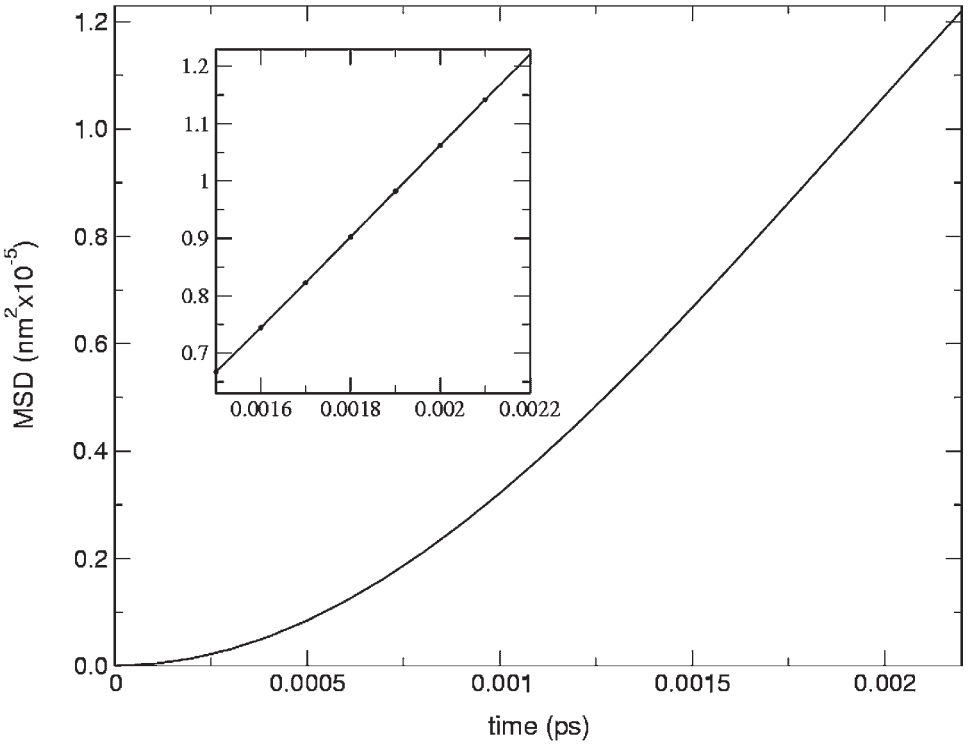

Figure 4. Mean square displacement (MSD) along the IRC as provided by the constant energy simulation of malonaldehyde in water (see Methods), used to obtain the reaction coordinate diffusion coefficient. No error bars are reported as the estimated noise is too small to be visible on the figure scale. In the inset we show the time range used to obtain the diffusion coefficient by fitting MSD data by a linear regression

energy simulation, providing $D = 4.1 \times 10^{-3} \pm 10^{-4}$ nm^2/ps (the noise indicated is the error upper limit). It is also interesting to note that the diffusive regime is accessed within 1 fs, indicating that the velocity autocorrelation function relaxation is extremely fast (in the inset we show the time range used to obtain the diffusion coefficient by fitting MSD data by a linear regression). By using such a diffusion coefficient and the (300 K) perturbed reaction free energy into the diffusion equation (DE), see Theory section, we could obtain the detailed time course of the proton transfer reaction from the reactant to the product state. In Fig. 5 we show the probability profile, along η, as provided by the (numerical) DE solution at three different times. In order to schematize the kinetic process, we used three chemical states according to Fig. 2: the transition state (TS), defined by a 0.01 nm IRC interval centered on the free energy maximum, the reactant (R), defined by the IRC range at left of the TS, and the product (P) defined by the IRC range at right of the TS. Hence, within such a scheme the complete reaction can be described by the time dependence of these three chemical state probabilities. In Fig. 6 we show the time courses of the three probabilities as obtained by the DE solution. R, and P probabilities converge to their equilibrium values within 120–150 ps, clearly indicating a rather fast kinetics. From the figure it is also clear that the TS reaches a stationary condition within $t_o = 300$ fs, providing in the following time range a completely symmetric reactant and product kinetics (i.e., identical relaxation rates and final equilibrium values), as expected by the free energy symmetric shape. Interestingly, the R and P relaxations, when subtracted of the equilibrium value, are perfectly exponential (beyond t_0) for virtually the complete reaction time course with a rate constant $K = 0.038 \pm 0.001$ ps^{-1} corresponding to the mean life $\tau \cong 26$ ps (the noise indicated is the error upper limit). Note that a different definition of the three states using short intervals (0.014 Å) centered on the two free energy minima (R and P states) and on the free energy maximum (TS state), provided a virtually identical rate constant and kinetic behavior. Remarkably, the obtained rate constant is well matching the experimentally observed kinetics of this reaction in solution[10,11] (picoseconds range in $CFC1_3$/CD_2C1_2) and suggests that tunneling might be not relevant in liquid phase conditions, as also indicated by the theoretical-computational estimate of the tunneling rate in liquid water[26] (nanoseconds range). Such a result, obtained in condensed phase, is also in agreement with the data obtained in a previous computational attempt to investigate malonaldehyde proton transfer in vacuum,[25] leading to similar conclusions for the gas phase reaction. It is also interesting to note that the use of standard Transition State Theory with unitary transmission coefficient provides a lower value of the rate constant (mean life of about 100 ps), showing that a more general kinetic model should be used to rationalize the DE results. On the basis of the results obtained by DE solution (Figs. 5 and 6) we may define (in strong analogy with Eyring approach) the R, P, and TS chemical states and the general reaction scheme

$$R \xrightarrow{k_1} TS \xrightarrow{k_{-2}} P \tag{17}$$

$$P \xrightarrow{k_2} TS \xrightarrow{k_{-1}} R \tag{18}$$

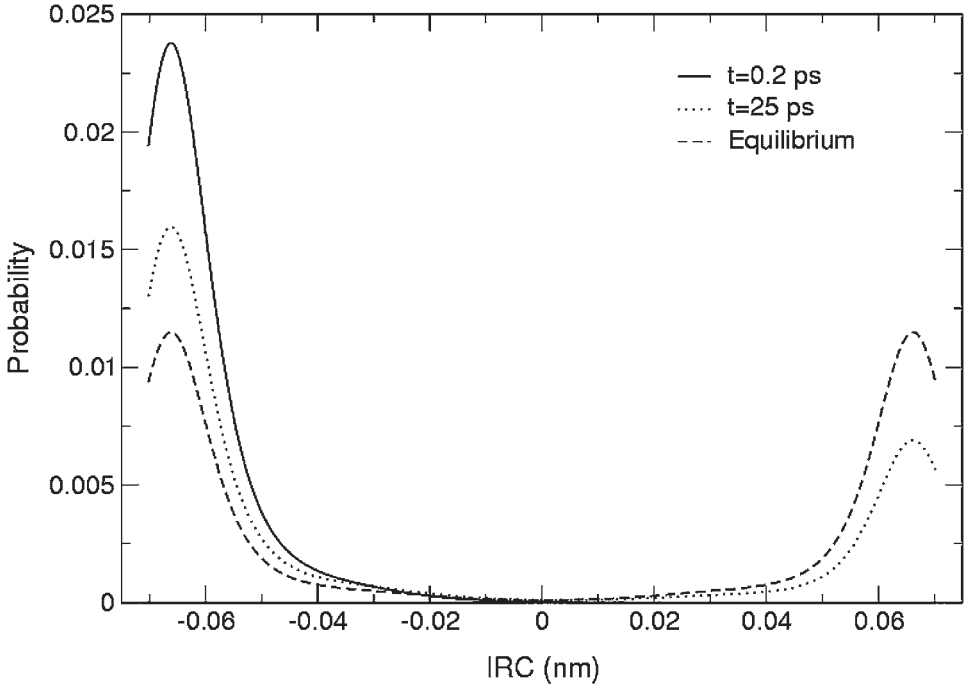

Figure 5. Probability distributions along IRC at three different times, as obtained by solving the diffusion equation

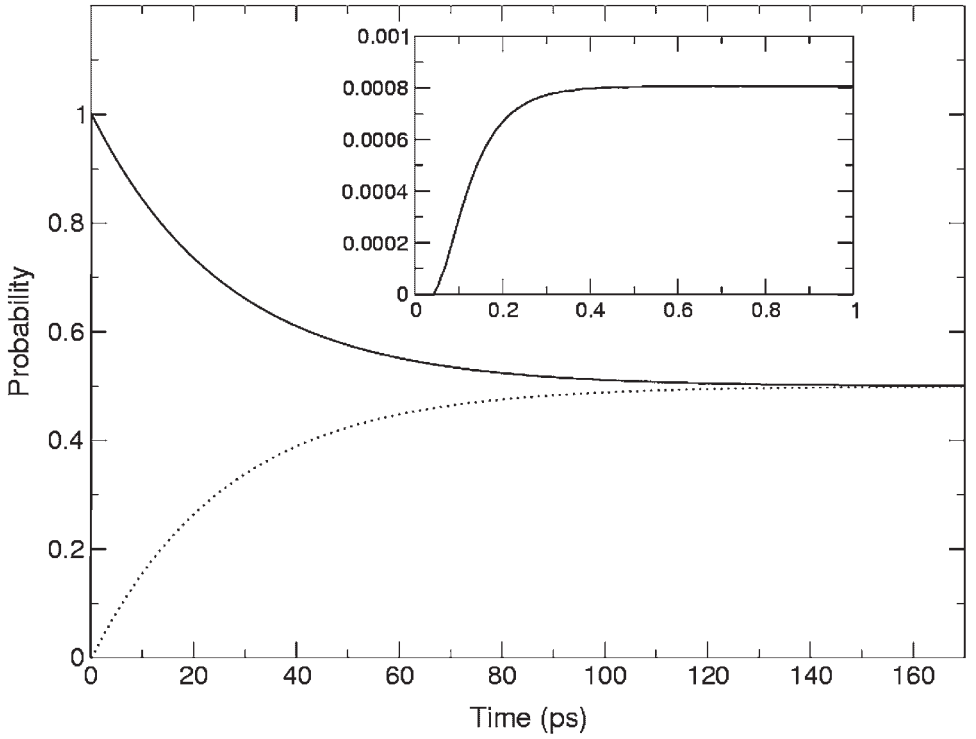

Figure 6. Time course of the reactant (solid line), product (dotted line) and transition state (inset) probabilities as obtained by solving the diffusion equation

Considering symmetric rate constants (due to the symmetric reaction free energy), that is

$$k_1 = k_2 = k_+$$

$$k_{-1} = k_{-2} = k_-$$

we obtain for $t \geq t_0$ (see the Appendix 1)

$$\frac{\mathrm{P}_R(t) - \mathrm{P}_R(\infty)}{\mathrm{P}_R(t_0) - \mathrm{P}_R(\infty)} \cong \mathrm{e}^{-K(t-t_0)} \tag{19}$$

$$\frac{\mathrm{P}_P(t) - \mathrm{P}_P(\infty)}{\mathrm{P}_R(t_0) - \mathrm{P}_R(\infty)} \cong -\mathrm{e}^{-K(t-t_0)} \tag{20}$$

$$P_{TS}(t) \cong P_{TS}(\infty) = \frac{k_+}{2k_- + k_+}$$

$$K = \frac{2k_+k_- + k_+^2}{2k_- + k_+} = k_+$$

where P_{R}, P_{P}, P_{TS} are the probabilities for R, P, and TS, respectively. Note that such a steady state model, based on the assumption $\dot{P}_{TS} \cong 0$ and matching perfectly the DE results in the $t \geq t_0$ range, is rather different from the Eyring model which assumes a pre-equilibrium between the R and TS species, considering only the $R \rightarrow P$ reaction (see the Appendix 1). Using the equilibrium TS probability as well as the $k_+ = K$ rate constant, we may also evaluate the inverse reaction constant $k_- = 23.4 \pm 0.6\,\mathrm{ps}^{-1}$ corresponding t_0 a mean life of about 43 fs (the noise indicated is the error upper limit).

Finally, in order to check the accuracy of our basic assumption that the IRC can be used as a single reaction coordinate to describe the proton transfer kinetics, we can monitor the perturbing electric field relaxation. In Fig. 7

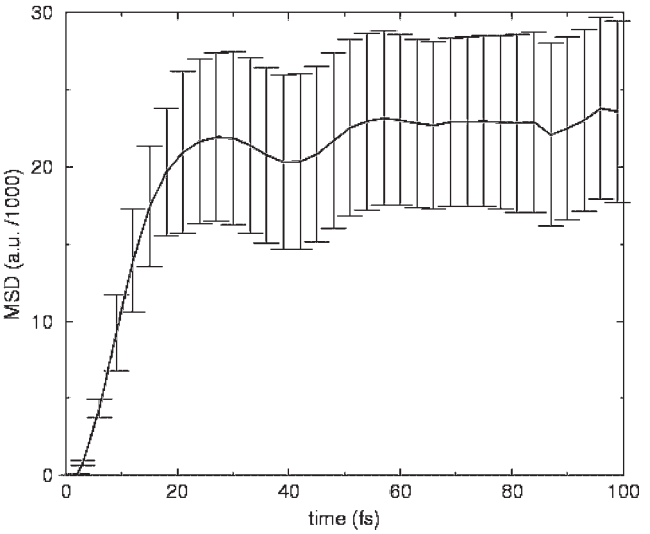

Figure 7. Mean square displacement (MSD) of the perturbing electric field, as obtained by the 300 K simulation. The error bars shown correspond to a standard deviation of the MSD

we show the mean square displacement in time of the perturbing field (defined in the malonaldehyde reference frame summing the MSD of each component), as obtained by the 300 K simulation considering a set of subtrajectories starting in the probability maximum of the field, that is, the free energy minimum in the field space. From the figure it is evident that the perturbation is fully relaxed within 20–30 fs, indeed showing that the solvent can be considered as instantaneously relaxed along the IRC transition occurring, as found by our model, within several tens of picoseconds.

CONCLUSIONS

In this paper we utilized the very recently introduced theoretical modeling of the reaction thermodynamics in complex systems,[38] to treat the intramolecular proton transfer of aqueous malonaldehyde. Comparison between solution (PMM) and vacuum reaction free energy profiles clearly shows that water acts as a 'catalyzator'' of the reaction, lowering the free energy barrier. Such a result is not a simple dielectric effect as PCM calculations provide essentially the same free energy barrier of the vacuum curve. Interestingly the solution reaction free energy surface, as obtained by PMM and MD simulations, shows a weak temperature dependence and the QGE model, constructed to describe the complete reaction thermodynamics, clearly indicates that no large entropic variations are involved in the proton transfer process although an entropy reduction is present in correspondence of the transition structure (negative activation entropy). The reaction free energy surface and the estimated diffusion coefficient along IRC were used in the diffusion equation to provide the complete (classical) kinetics of the reaction. The accuracy of such a theoretical evaluation of the kinetics, based on the assumption that all the degrees of freedom orthogonal to the reaction coordinate are instantaneously relaxed during the IRC transition, has been checked by evaluating the relaxation rate of the perturbing electric field, resulting more than 1000 times faster than the IRC transition rate as obtained by the model itself. In fact the obtained proton transfer kinetics, providing a transition rate constant of $0.038\,ps^{-1}$, fits well the experimentally estimated picoseconds range transition mean time in $CFC1_3$/CD_2C1_2 solution,[10,11] that is, the only available experimental data on the reaction in condensed phase found in literature. This result, when considering the much larger tunneling mean life in aqueous solution as provided by theoretical-computational data,[26] suggests that tunneling could be kinetically not relevant in condensed phase, as also reported for the gas-phase reaction.[25] Finally, our data show that Eyring theory is inaccurate in the present case and a more general chemical kinetic model must be used to rationalize the diffusion equation results (see Appendix 1).

Acknowledgements

We gratefully acknowledge Dr N. Tantalo and 'Centro Ricerche Studi Enrico Fermi' (Roma, Italia) for computational support. We also thank CASPUR (Roma, Italia) for allowing us to use Gaussian98. Renato Di Bartolomeo (Universita' di L'Aquila) is also acknowledged for his help in the preparation of the manuscript.

APPENDIX 1

Consider the general reaction scheme for the three chemical states R, P and TS

$$R \xrightarrow{k_1} TS \xrightarrow{k_{-2}} P \tag{21}$$

$$P \xrightarrow{k_2} TS \xrightarrow{k_{-1}} R \tag{22}$$

and the stationary condition

$$\dot{P}_{TS} = k_1 P_R - k_{-1} P_{TS} + k_2 P_P - k_{-2} P_{TS} \cong 0 \tag{23}$$

$$P_{TS} \cong \frac{k_1 P_R + k_2 P_P}{k_{-1} + k_{-2}} \tag{24}$$

valid for $t \geq t_0$ (t_0 is the time interval required to achieve the steady state). From the relation $1 = P_R(0) = P_R(t) + P_P(t) + P_{TS}(t)$ we have $P_P(t) = 1 - P_R(t) - P_{TS}(t)$ and hence $\forall t \geq t_0$

$$P_{TS}(t) \cong \frac{(k_1 - k_2)P_R + k_2}{k_{-1} + k_{-2} + k_2} \tag{25}$$

$$\dot{P}_R \cong -KP_R + K' \tag{26}$$

$$K = \frac{k_1 k_{-2} + k_1 k_2 + k_2 k_{-1}}{k_{-1} + k_{-2} + k_2} \tag{27}$$

$$K' = \frac{k_2 k_{-1}}{k_{-1} + k_{-2} + k_2} \tag{28}$$

The general solution of the previous ordinary linear differential equation is, in the time range $t \geq t_0$,

$$P_R(t) \cong P_R(\infty) + [P_R(t_0) - P_R(\infty)]e^{-K(t-t_0)} \tag{29}$$

$$P_R(\infty) = \frac{K'}{K} = \frac{k_2 k_{-1}}{k_1 k_{-2} + k_1 k_2 + k_2 k_{-1}}$$

From the last expressions we readily obtain (using again $P_P(t) = 1 - P_R(t) - P_{TS}(t)$ and the stationary

condition)

$$P_P(t) \cong P_P(\infty) - \frac{k_{-1}+k_{-2}+k_1}{k_{-1}+k_{-2}+k_2} + [P_R(t_0) - P_R(\infty)]\mathrm{e}^{-K(t-t_0)} \quad (30)$$

$$P_P(\infty) = \frac{k_{-1}+k_{-2}-(k_{-1}+k_{-2}+k_1)P_R(\infty)}{k_{-1}+k_{-2}+k_2} = \frac{k_1 k_{-2}}{k_1 k_{-2}+k_1 k_2+k_2 k_{-1}}$$

$$P_{TS}(t) \cong P_{TS}(\infty) + \frac{k_1-k_2}{k_{-1}+k_{-2}+k_2}[P_R(t_0) - P_R(\infty)]e^{-K(t-t_0)} \quad (31)$$

$$P_{TS}(\infty) = \frac{(k_1-k_2)P_R(\infty)+k_2}{k_{-1}+k_{-2}+k_2} = \frac{k_1 k_2}{k_1 k_{-2}+k_1 k_2+k_2 k_{-1}}$$

When in the P_R, P_p, P_{TS} expressions we use symmetric rate constants, that is, $k_1 = k_2 = k_+$, $k_{-1} = k_{-2} = k_-$, we obtain the relations, given in the Results and Discussion section, valid for the aqueous malonaldehyde proton transfer. It is also instructive to consider other two special cases of this general model. If we deal with a reaction where $k_2 \cong 0$ then we have $K \cong k_1 k_{-2}/(k_{-1}+k_{-2})$ and

$$\frac{P_{TS}}{P_R} \cong \frac{k_1}{k_{-1}+k_{-2}} \quad (32)$$

corresponding to a simple steady state for the $R \to P$ reaction alone. This case is typical in systems where the free energy of the product is much lower than the reactant one or the product is instantaneously removed in some way (e.g., in enzymatic reactions). When $k_2, k_{-2} \cong 0$ we obtain a further condition with $K \cong k_1 k_{-2}/k_{-1}$ and $P_{TS}/P_R \cong k_1/k_{-1}$ which clearly corresponds to a pre-equilibrium between the R and TS species, as required by the Eyring theory. However, this last case is rather unusual as k_{-2} is typically larger or of the same order of k_{-1} when $k_1 \gg k_2$, and hence Eyring theory should not be used as a general model to describe chemical reactions.

APPENDIX 2

In this appendix we show, in a simple and direct way, how to obtain the diffusion equation used in this paper.

'Consider, in general, a set of reaction coordinates η providing the kinetic relaxation of the system, that is, all the other degrees of freedom are assumed to be fully equilibrated along the η relaxation. The equations of motion for the η degrees of freedom when averaging over the ensemble defined by the solute molecules within a tiny η volume (equivalent to a numerical differential), can be approximated as

$$\langle \dot{\pi}_\eta(\eta) \rangle \cong F(\eta) - \tilde{\mathbf{\Gamma}}(t,\eta)\langle \pi_\eta(\eta) \rangle \quad (33)$$

$$\langle \pi_\eta(\eta) \rangle = \tilde{\mathbf{M}}_{\eta,\eta}(\eta)\langle \dot{\eta}(\eta) \rangle \quad (34)$$

where π_η are the η conjugated momenta, F is the systematic, that is, equivalent to an external field, force in the space and $\tilde{\mathbf{\Gamma}}$, $\tilde{\mathbf{M}}_{\eta,\eta}$ are the friction matrix and solute (classical) mass tensor block corresponding to the η coordinates. We assumed a virtually fixed solute mass tensor for a given η position and hence $\tilde{\mathbf{M}}_{\eta,\eta}$ provides the only non zero terms of π_η after averaging, as the other degrees of freedom are considered as fully equilibrated with hence zero mean velocities. Within the approximation given by the previous equations, the work due to the systematic force only should coincide with the maximum work along the transition, that is, the work obtained for a reversible transition with then $\langle \dot{\eta} \rangle = 0$. Hence, for a molecule passing from a tiny volume centered at η_a to another one centered at η_b we can write

$$\Delta A(\mathbf{n}) = \left(\frac{\partial A}{\partial n_{\eta_b}}\right) + \left(\frac{\partial A}{\partial n_{\eta a}}\right)\left(\frac{\partial n_{\eta a}}{\partial n_{\eta b}}\right) = \mu(n_{\eta_b}, \eta_b) - \mu(n_{\eta a}, \eta_a) = -\int_{\eta_a}^{\eta_b} F(\eta)\cdot d\eta \quad (35)$$

providing

$$F(\eta) = -\nabla\eta\mu(n_\eta, \eta) \quad (36)$$

In the last equations $A(\mathbf{n})$ is the Helmholtz free energy of the total NVT system fully defined by the vector $\mathbf{n} = n_{\eta_1}, n_{\eta_2}, \ldots$ providing the solute molecular number in each tiny volume and $\mu(n\eta, \eta)$ is the chemical potential at a given η position, that is, within the corresponding tiny volume. Note that the molecular number can be used as a continuous variable, given the fact that for any thermodynamic property in a macroscopic system the variation due to a single molecule is virtually equivalent to a differential. From the definition of the chemical potential and solute density in the η space $\rho(t,\eta)$, we readily have

$$\mu(n_\eta, \eta) = \Delta\mu^{\ominus}(\mathbf{n}) + kT\ \ln\frac{n_\eta}{n_{\eta R}} + \mu(n_{\eta R}, \eta_R) \quad (37)$$

$$= \Delta\mu^{\ominus}(\mathbf{n}) + kT\ \ln\frac{\rho(t,\eta)}{\rho(t,\eta_R)} + \mu(n_{\eta R}, \eta_R) \quad (38)$$

which used together with $\langle \dot{\pi}_\eta \rangle \cong 0$ (the linear regime condition) provides

$$\langle \dot{\eta}(\eta) \rangle \cong -\left[\tilde{\mathbf{\Gamma}}(t,\eta)\tilde{\mathbf{M}}_{\eta,\eta}(\eta)\right]^{-1}\nabla\eta\Delta\mu^{\ominus}(\mathbf{n}) - \left[\tilde{\mathbf{\Gamma}}(t,\eta)\tilde{\mathbf{M}}_{\eta,\eta}(\eta)\right]^{-1} kT\frac{\nabla\eta\rho(t,\eta)}{\rho(t,\eta)} \quad (39)$$

Hence from the definition of the flux density vector $\mathbf{J}(\eta) = \rho(t,\eta)\langle\dot{\eta}(\eta)\rangle$ and setting

$$\tilde{D}(t,\eta) = kT\left[\tilde{\mathbf{\Gamma}}(t,\eta)\tilde{\mathbf{M}}_{\eta,\eta}(\eta)\right]^{-1} \tag{40}$$

we obtain, via the divergence theorem,

$$\left(\frac{\partial\rho}{\partial t}\right)_{\eta} = -\nabla\eta\cdot\mathbf{J} \cong \nabla\eta\cdot\left[\tilde{D}(kT)^{-1}\rho\nabla\eta\Delta\mu^{\ominus}\tilde{D}\nabla\eta\rho\right] \tag{41}$$

This last equation, when considering a one dimensional η space with then $\tilde{D} = D$, provides the diffusion equation used in this paper within the assumption $\partial D/\partial t, \partial D/\partial\eta \cong 0$ (see theory section).'

REFERENCE

1. Gonzales C, Schlegel HB. *J. Chem. Phys*. 1989; **90**: 2154.
2. Barone V, Adamo C. *J. Chem. Phys*. 1996; **105**: 11007.
3. Bauer SH, Wilcox CF. *Chem. Phys. Lett*. 1997; **279**: 122.
4. Sadhunkhan S, Munoz D, Adamo C, Scuseria C. *Chem. Phys. Lett*. 1999; **306**: 84.
5. Buemi G. *Chem. Phys*. 2002; **277**: 241.
6. Sewell TD, Guo Y, Thompson DL. *J. Chem. Phys*. 1995; **103**: 8557.
7. Smedarchina Z, Fernandez-Ramos A, Rios MA. *J. Chem. Phys*. 1997; **106**: 3956.
8. Iftimie R, Schofield J. *J. Chem. Phys*. 2001; **115**: 5891.
9. Tautermann CS, Voegele AF, Loerting T, Liedl KR. *J. Chem. Phys*. 2002; **117**: 1962.
10. Brown SR, Tse A, Nakashima T, Haddon RC. *J. Am. Chem. Soc*. 1979; **101**: 3157.
11. Perrin CL, Kim YJ. *J. Am. Chem. Soc*. 1998; **120**: 12641.
12. Seliskar CJ, Hoffmann RE. *J. Mol. Spectr*. 1982; **96**: 146.
13. Frith DW, Barbal PF, Trommsdorf HF. *Chem. Phys*. 1989; **136**: 349.
14. Chivassa T, Verlaque P, Allouche A, Marinelli F. *J. Phys. Chem*. 1992; **96**: 10659.
15. Baughcum SL, Duerts RW, Rowe WF, Smith Z, Wilson EB. *J. Am. Chem. Soc*. 1981; **103**: 6296.
16. Baughcum SL, Smith Z, Wilson EB, Duerts RW. *J. Am. Chem. Soc*. 1984; **106**: 2260.
17. Duan C, Luckhaus D. *Chem. Phys. Lett*. 2004; **391**: 129.
18. Bothner-By A, Harris RK. *J. Org. Chem*. 1965; **30**: 254.
19. George WO, Mansell VG. *J. Chem. Soc. (B)*: 1968; 132.
20. Bertz SH, Dabbagh G. *J. Org. Chem*. 1990; **55**: 5161.
21. Tomasi J, Persico M. *Chem. Rev*. 1994; **94**: 2027.
22. Berendsen HJC, Mavri J. *J. Phys. Chem*. 1993; **97**: 13464.
23. Borgis D, Hynes JT. *J. Chem. Phys*. 1991; **94**: 3619.
24. Garcia-Viloca M, Alhambra C, Truhlar DG, Gao J. *J. Chem. Phys*. 2001; **114**: 9953.
25. Wolf K, Mikenda W, Nusterer E, Schwartz K, Ulbricht C. *Chem. Eur. J*. 1998; **4**: 1418.
26. Mavri J, Berendsen HJC, van Gunsteren WF. *J. Phys. Chem*. 1993; **97**: 13469.
27. Naka K, Sato H, Morita A, Hirata F, Kato S. *Theor. Chem. Acc*. 1999; **102**: 165.
28. Wesoloski TA, Muller RP, Warshel A. *J. Phys. Chem*. 1996; **100**: 15444.
29. Fdez-Galvan I, Martin ME, Aguilar MA. *J. Comp. Chem*. 2004; **25**: 1227.
30. See for example: (a) Kormos BL, Cramer CJ. *J. Org. Chem*. 2003; **68**: 6375; (b) Cammi R, Mennucci B, Tomasi J. *J. Phys. Chem. A*: 1999; **103**: 9100.
31. Aschi M, Spezia R, Di Nola A, Amadei A. *Chem. Phys. Lett*. 2001; **344**: 374.
32. Spezia R, Aschi M, Di Nola A, Amadei A. *Chem. Phys. Lett*. 2002; **365**: 450.
33. Spezia R, Aschi M, Di Nola A, Valentin MD, Carbonera D, Amadei A. *Biophys. J*. 2003; **84**: 2805.
34. Amadei A, Zazza C, D'Abramo M, Aschi M. *Chem. Phys. Lett*. 2003; **381**: 187.
35. Aschi M, Zazza C, Spezia R, Bossa C, Di Nola A, Paci M, Amadei A. *J. Comput. Chem*. 2004; **25**: 974.
36. D'Abramo M, Aschi M, Di Nola A, Amadei A. *Chem. Phys. Lett*. 2005; **402**: 559.
37. Aschi M, D'Abramo M, Di Teodoro C, Di Nola A, Amadei A. *Chem. Phys. Chem*. 2005; **6**: 53.
38. Amadei A, D'Alessandro M, Aschi M. *J. Phys. Chem. B*: 2004; **108**: 16250.
39. D'Alessandro M, Aschi M, Paci M, Di Nola A, Amadei A. *J. Phys. Chem. B*: 2004; **108**: 16255.
40. D'Abramo M, D'Alessandro M, Amadei A. *J. Chem. Phys*. 2004; **120**: 5226.
41. Truhlar DG, Garrett BC, Klippenstein SJ. *J. Phys. Chem*. 1996; **100**: 12771.
42. Baer T, Hase WH. *Unimolecular reaction dynamics*. Oxford University Press: Oxford, 1996.
43. Miller WH, Handy NC, Adams JE. *J. Chem. Phys*. 1980; **72**: 99.
44. Kato S, Morokuma KJ. *J. Chem. Phys*. 1980; **73**: 3900.
45. In this paper we do not consider reactive processes which may relax faster or at a similar rate than the environment as for a simple molecule like malonaldehyde, they typically may occur at very high temperature. However, for more complex molecules involving slowly relaxing internal coordinates, for example, biomacromolecules, it is possible that such slow modes must be somehow included in the definition of the reactive surface in order to describe properly the kinetics of the reaction and not only its thermodynamics.
46. Amadei A, Marinelli F, D'Abramo M, D'Alessandro M, Anselmi M, Di Nola A, Aschi M. *J. Chem. Phys*. 2005; **122**: 124506.
47. McQuarrie DA. *Statistical mechanics*. Harper Collins Publishers: New York, 1976.
48. Becke AD. *J. Chem. Phys*. 1986; **84**: 4524.
49. Lee C, Yang NV, Parr RG. *Phys. Rev. B*: 1988; **37**: 785.
50. Krishnan R, Binkley JS, Seager R, Pople JA. *J. Chem. Phys*. 1980; **72**: 650.
51. Pople JA, Head-Gordon M, Raghavachari K. *J. Chem. Phys*. 1997; **87**: 5968.
52. Casina ME, Jamorski C, Casina KC, Salahub DR. *J. Chem. Phys*. 1998; **108**: 4439.
53. Gaussian 98 (Revision A.7), Gaussian, Inc.: Pittsburgh PA, 1998.
54. Feenstra KA, Hess B, Berendsen HJC. *J. Comput. Chem*. 1999; **20**: 786.
55. Spackman MA. *J. Comput. Chem*. 1996; **17**: 1.
56. Darden TA, York DM, Pedersen LG. *J. Chem. Phys*. 1993; **98**: 10089.
57. van der Spoel D, van Drunen R, Berendsen HJC, ''GRoningen MAchine for Chemical Simulations'', Department of Biophysical Chemistry, BIOSON Research Institute, Nijenborgh 4 NL-9717 AG Groningen, 1994 e-mail to gromacs@chem.rug.nl.
58. van der Spoel D, van Buuren AR, Apol E, Meulenhoff PJ, Tieleman DP, Sijbers ALTM, van Drunen R, Berendsen HJC, ''Gromacs User Manual Version 1.3'', Internet: http://rugmdO.chem.rug.nl/gmx 1996.
59. van Gunsteren WF, Billeter SR, Eising AA, Hunenberger PH, Kruger P, Mark AE, Scott WVRP, Tironi IG. *Biomolecular simulation: The GROMOS96 Manual and User Guide*. Hochschulverlag AG an der ETH Zurich: Zurich, 1996.
60. Hess B, Bekker H, Berendsen HJC, Fraajie H. *J. Comp. Chem*. 1997; **18**: 1463.
61. Amadei A, Chillemi G, Ceruso MA, Grottesi A, Di Nola A. *J. Chem. Phys*. 2000; **112**: 9.
62. Evans DJ, Morriss GP. *Statistical mechanics of nonequilibrium liquids*. Academic Press: London, 1990.
63. D'Alessandro M, Tenenbaum A, Amadei A. *J. Phys. Chem. B*: 2002; **106**: 5050.